

**A computational model to predict antibiotic
susceptibility of *Pseudomonas aeruginosa*
Biofilms**

R Anil

A Thesis Submitted to
Indian Institute of Technology Hyderabad
In Partial Fulfillment of the Requirements for
The Degree of Master of Technology



भारतीय प्रौद्योगिकी संस्थान हैदराबाद
Indian Institute of Technology Hyderabad

Department of Chemical Engineering

June 2014

Declaration

I declare that this written submission represents my ideas in my own words, and where ideas or words of others have been included, I have adequately cited and referenced the original sources. I also declare that I have adhered to all principles of academic honesty and integrity and have not misrepresented or fabricated or falsified any idea/data/fact/source in my submission. I understand that any violation of the above will be a cause for disciplinary action by the Institute and can also evoke penal action from the sources that have thus not been properly cited, or from whom proper permission has not been taken when needed.

R. Anil

(Signature)

R. ANIL

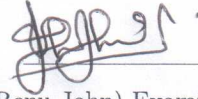
(R Anil)

CH12M11012

(Roll No.)

Approval Sheet

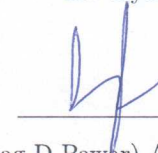
This Thesis entitled A computational model to predict antibiotic susceptibility of *Pseudomonas aeruginosa* Biofilms by R Anil is approved for the degree of Master of Technology from IIT Hyderabad.



(Dr. Renu John) Examiner
Dept. of Biomedical Eng
IIT Hyderabad



(Dr. Phanindra Jampana) Examiner
Dept. Chemical Eng
IIT Hyderabad



(Dr. Parag D Pawar) Adviser
Dept. of Chemical Eng
IIT Hyderabad



(Dr. Dayadeep Monder) Chairman
Dept. of Chemical Eng
IIT Hyderabad

Acknowledgements

Apart from the complete involvement and efforts of me, first and foremost I take this opportunity to express my profound gratitude and deep regards to my advisor Dr. Parag D. Pawar for his exemplary guidance, motivation, monitoring and constant encouragement in the successful completion of this thesis work.

I would like to thank my committee members, Dr. Renu John, Dr Dayadeep Monder, and Dr Phanindra J ampana for their insightful comments and valuable advises during project work progress discussions.

My sincere thanks to Anitha Mogilicharla for her generous help during MATLAB visuals development and also would like to extend my thanks to Mr. Teja and Mr. Tejesh for allowing me to use their high performance computing facility accounts.

My special thanks to Lakshmi Machineni, Pinakinarayan A. P. Swain, Vudikala Chaitanya, Goutham Polisetty, Ritwika Raha for their moral support and cooperation during my research work.

I am grateful to the office staff of computer lab, IITH for providing excellent computation facilities to complete this project.

I am also thankful to my parents, brother and sister who always encouraged and supported in every stage of my life.

Finally I would like to thank my friends and several individuals with whom this dissertation would not have been possible for their guidance in one way or another contributed and extended their valuable assistance in the preparation and completion of this study.

Abstract

A Three dimensional cellular automata model to predict antibiotic susceptibility of *Pseudomonas aeruginosa* biofilms has been developed. This model integrates the process of substrate transport and utilisation, biomass growth, biomass division and spreading, cell death and detachment, EPS production, quorum sensing and antimicrobial drug administrative killing. There are different mechanisms of antibiotic resistance of bacterial population in biofilm mode of growth have been reported such as, depletion of antimicrobial agents by reaction with biomass or physiological resistance due to reduced bacterial growth in the biofilm, etc.. Our model investigated the biofilm susceptibility depending upon the growth rate of microbial population and concentration of antibiotic during antimicrobial treatment. Bacterial growth rate effects on microbial mat resistance studied using two different substrate concentrations 3 gm m^{-3} and 5 gm m^{-3} . To study antibiotic concentration dependent killing, *Pseudomonas aeruginosa* biofilms were grown in 3 gm m^{-3} nutrient concentration with three antimicrobial concentrations. Antibiotic agent concentration was varied from 0 gm m^{-3} to 10 gm m^{-3} to observe *Pseudomonas aeruginosa* biofilms susceptibility. Antimicrobial therapy was initiated at 40th hour of biofilm simulation and continued for next 48 hours. Biofilm developed under low nutrient concentration treated with low concentration of antibiotic shows an extended life cycle having a smoother and compact structure than untreated biofilm matrix, while upon treatment with high concentration of antibiotic, bacterial cell death happens for the same biofilm. In untreated biofilm cell death starts at bottom core of the biofilm whereas in treated biofilms cell death happens at top surface of the biofilm. Biofilm grown under high substrate concentration died faster, forms a rougher surface whereas biofilms grown under low substrate concentration retains viable for prolonged time, forms very compact structure.

Contents

Declaration	ii
Approval Sheet	iii
Acknowledgements	iv
Abstract	v
Nomenclature	vi
1 Introduction	1
2 Literature Review	4
3 Methods	8
3.1 Biofilm simulation domain geometry	8
3.2 Substrate transport and transformation	9
3.3 Rate of biomass production	10
3.4 Cell division	10
3.5 Cell death	10
3.6 Cell detachment	11
3.7 EPS Production	11
3.8 Quorum sensing	12
3.9 Autoinducer transport and transformation	13
3.10 Antimicrobial drug administration and killing	13
4 Results and Discussions	16
4.1 Antibiotic concentration dependent Biofilm resistance	22
4.2 Growth rate dependent Biofilm resistance	26
5 Conclusion	29
References	30

Chapter 1

Introduction

At any given time bacteria which are good to human host perform vital functions in the body. While some bacteria which are pathogenic to human body implicated in to a vast number of diseases ranges from a mild non-healing wounds to life threatening endocarditis [1, 2].

It has been well understood that microbial population can switch from a free-living state to a sessile mode of life to form harmful and antimicrobial tolerant biofilms embedded in a self-produced thick gel-like layers of extracellular polymeric substances(EPS) [3, 4]. Aside from polysaccharides, EPS matrix also consists of lipids, nucleic acids, proteins, extracellular DNA and adhesive fibers acts as a stabilizing scaffold for the three-dimensional biofilm structure [5]. The thickness of the EPS layer doesnt exceed 0.1 to 1.0 μ m. Depending on the age and different environmental conditions under which the microbial mat exists, composition of the EPS will vary [5].

The development of biofilm is a series of complex but distinct and well-regulated genetic mechanism differ from organism to organism. The attachment of a small number of living cells anywhere along the system is all that is needed to initiate biofilm formation. Within few minutes, the adherent cells undergo exponential binary division. The new daughter cell spread upward from the attachment points, and embeds in EPS to form micro colonies. Microcolonies are mainly comprised of 10% to 25% cells and 75% to 90% EPS matrix [6, 7, 8].

The biofilm structural and metabolic heterogeneity is influenced by intercellular signaling known as quorum sensing, in reaction to availability of nutrients in the immediate environment and growth conditions. Quorum sensing induces changes in bacterial gene expression that aim to promote cell growth rate regulation, cell-cell interaction, and toxin production [9, 10]. The multilayered cell clusters may develop as patchy networks or form a continuous layer over substratum depending on initial number of attached cells. Expanded cellular density evolves in to complex 3-D structure of smooth, fuzzy tower or mushroom-shaped cell clusters or tulip-like protrusions depending on the species and local environment. Additionally viscoelasticity property of biofilm allows them to deform structurally when exposed to varying shear stresses [11].

Biofilms can be made up of single microbial species or poly microbial species on a range of biotic and abiotic surfaces [12, 13]. Although mixed microbial species biofilm prevail in most environments, single species biofilm exist in a variety of infections and on the surface of indwelling medical implants (e.g., central venous catheters and needleless connectors, contact lenses, mechanical heart valves) [5, 13]

The primary opportunistic pathogens frequently involved in medical device contamination and developing biofilm-associated infections in immunocompromised host include Gram-positive bacteria (especially *streptococci* and *staphylococci*), Gram-negative bacteria (especially *Pseudomonas aeruginosa*, *Escherichia coli* and *Klebsiella pneumoniae*) and fungi (especially *Candida spp.* and *Aspergillus spp.*). Biofilm-associated infections caused by a single microbial species are the focus of most current research [14, 15]. Biofilm forming bacteria receiving major concern from clinicians in the treatment of infectious diseases because of their resistance to a wide range of antimicrobial agents [3].

Pseudomonas aeruginosa is an important gram-negative pathogen and avid biofilm former can cause native acute and chronic lung infections with significant morbidity and mortality, especially in cystic fibrosis patients [16]. Earlier studies shown that, presence of neutrophils in the cystic fibrosis airway enhances initial *P.aeruginosa* biofilm development over a period of 72 h thorough the formation of polymeric framework comprised of neutrophil-derived DNA and F-actin [17, 18, 19, 20, 21]. *Pseudomonas aeruginosa* is an opportunistic pathogen which is a difficult target for all classes of antimicrobial agents [22].

Bacterial surface immobilization as a biofilm provides sheltered architecture allowing cells to communicate, and creates a nutrient source pool from lysed cells. Biofilm mode of growth strengthens the microbial cells and protects them from host immune defense, repeated dosing of different antibiotics, radiation and oxidizing or charged biocides [13]. It is widely accepted that sessile bacteria community can be up to 800-1000 fold more resistant to antibiotic stress than the same organism planktonic counterparts and are much difficult to eradicate [23].

The reduced antimicrobial chemotherapy susceptibility of attached bacteria gains particular concern in gram-negative bacterial population where there is an insufficiency of new and effective antimicrobial agents [24, 25]. The surface-attached growth of bacterial community is promoting feature of many medical infections including dental caries, pneumonia in cystic fibrosis patients, urinary tract infections, and infections related medical implants and cardiac and vascular catheters [24].

Biofilm development includes number of sequential stages such as nutrient diffusion, microbial growth and expansion, EPS production to tailor the biofilm structure, quorum sensing, cell death and active dispersal occur simultaneously over a vast range of spatial and time scales. Although many times biofilms have harmful effects, they also offer huge potential for certain applications, such as bio-remediating hazardous waste sites, bio-filtering municipal and industrial water and wastewater, and forming bio-barriers to protect soil and groundwater from contamination [26, 27, 28]. Biofilms have been used successfully in water and wastewater treatment for over a century. Biofilm reactors can be used in full-scale applications for industrial and municipal waste-water treatment [29, 30]. While adverse effects of biofilm include their involvement in wide variety of acute infections, marked recalcitrance towards antimicrobial treatments, production of endotoxins and industrial fouling [31].

Biofilm formation achieved as a result of nutrient conversion, large number of biological (bacterial cell growth and division, production of extracellular polymers, and cell-cell signaling), chemical (mass transport) and physical phenomena (molecular diffusion and convection) over a broad range of length and time scales [27, 32, 33]. Biofilm architecture plays a key role in their function. Bacterial cell division and spreading, secretion of microbial exopolymers, hydrodynamic shear forces and regulated microbial detachment due to quorum sensing or nutrient starvation shape the structure of microbial sessile community. In order to utilize and control biofilms associated effects, relationship between

biofilm structure, their activity and other physiological attributes elucidation is crucial [32, 34].

Biofilms are involved in about 80% of bacterial associated infections in humans. Because of the challenging experimental measurements and dynamic nature of natural biofilms, mathematical modelers are trying to explain the physical and biological mechanism to determine how biofilm grow and how they contribute to antibiotic resistance by numerical simulations. Although there are many different ways of relating mathematical models to natural systems, biofilm models are mainly divided in to two main categories based on the biomass spreading mechanism. One subclass includes cell-centered discrete biofilm models (cellular automata or individual-based models), in which individual description of microbial cells under a set of rules used for biomass spreading. The other subclass is continuum models, where biomass spreading is modeled by partial differential and differential equations [8, 35].

Biofilm structure affected by various factors like cell detachment, EPS production, cell growth, hydrodynamic shear stress and cell death. Fagerlind et al., 2012 investigated the role of cell death in biofilm in a 2D system, which is not physically relevant. The objective of this study was to model biofilm growth in 3D which includes cell growth, cell division, cell death, attachment and detachment of cell, EPS production, cell-signaling process, and antimicrobial therapy.

The discretestochastic approach cellular automata embodied in our model provide a multiscale frame work for various ongoing processes and examine their impact in biofilm morphology. We constructed cellular automaton biofilm model from sub models, each of which solves ongoing phenomena in a biofilm development, including (i) substrate transport and molecular diffusions reactions, (ii) biomass growth and exponential binary division, (iii) biomass spreading and attachment, (iv) liquid flow environment effects on the biofilm, (v) EPS production, (vi) quorum sensing, (vii) Antimicrobial drug administration and killing, and (viii) biomass decay and detachment.

Chapter 2

Literature Review

Biofilm is a microbial derived sessile community characterized by cells that are irreversibly attached to an abiotic or living surface and embedded in a matrix of extracellular polymeric substances that they have produced. These biofilms behave differently from planktonic microorganisms [8]. This form clusters by producing an extracellular polymeric substance, also known as EPS. The cells are held together by these EPS and develop complex three-dimensional, resilient communities. These clusters of microorganisms excrete a glue-like substance, which allows them to adhere to a surface.

Biofilm growth starts when bacterial cell attaches to a surface which is exposed aqueous medium. Then microbes starts growing on the attached surface and produce EPS, which represents the house of the biofilm cells. The poly hydroxyl groups in EPS anchor the bacteria in the biofilm to the surface through hydrogen bonding. At this time, the microbes can no longer move away from the surface. Mature biofilms are anchored to their place until the final stage of growth. The cells in biofilm uptake nutrient available in environment and divides after appropriate growth, as a result of which biofilms grows [13]. This complex, dynamic systems represents a protected mode of growth that allows cells to survive in hostile environments and also disperse to form secondary colonies [36]. These comparatively more resistance to antibiotics [11, 37] as well as heavy metals [30], than individual planktonic cells. Biofilm associated infections in humans such chronic lung infection in cystic fibrosis patients, periodontitis, and various nosocomial infections share common characteristics is that bacteria in biofilms evade host defenses and with stand antimicrobial stress even though the microbial causes and host sites vary greatly [38]. Initially, penicillin was the extremely efficient antimicrobial agent in combating infections in immunocompromised patients. But as a results of bad administering approach, many bacterial strains like *S. aureus*, *K. pneumoniae*, were observed to gain resistance due to their adopted resistance genes [39, 40, 41].

Biofilm development involves different biological, chemical and physical processes, can be characterized using distinct spatial and temporal scales. Processes changing the biofilm volume (biomass growth, cell death and cell detachment) are much slower than processes involved in substrate mass balance (diffusion and convection). While momentum transport by convection is much faster than substrate mass transfer. Hence, it is justified to work at three time scales:

- 1) Biomass growth, in the order of hours or days.
- 2) Mass transport of solutes, in the order of minutes, and
- 3) Hydrodynamic processes, in the order of seconds.

There are many possible antibiotic resistance phenomena that have been elucidated in the literature. One of the possible hypothesis is incomplete antimicrobial penetration in to biofilm matrix. Even though there is no generic barrier to antibiotic molecular diffusion, penetration can be profoundly retarded due to a neutralizing reaction between the antimicrobial agent and some component of the biofilm. For example, ampicillin can penetrate through a biofilm formed by a β -lactamase-negative strain of *K pneumoniae* but not a biofilm formed by the β -lactamase-positive wildtype strain of the same micro-organism [42, 43, 44]. Another possible hypothesis of antibiotic resistance is altered internal micro environment of biofilm, like oxygen gradients, pH differences, osmotic stress and depletion of a substrate or accumulation of an inhibitive waste product might cause some bacteria to enter a non-growing state, in turn antagonise the action of an antibiotic. Penicillin antibiotics, which target cell-wall synthesis, kill only growing bacteria. Aminoglycoside antibiotics are clearly less effective against the same micro-organism in anaerobic than in aerobic conditions. Pathogenesis of *P. aeruginosa* is attributed to the production of several cell-associated and extracellular virulence factors that arise under certain environmental conditions [18]. A third hypothesis has been proposed that a small population of micro-organisms in a biofilm forms a unique, and highly protected, phenotypic state called 'persister cells', provides a powerful, and generic, explanation for the reduced susceptibility of biofilms to antibiotics and disinfectants. Survivors, which might consist of 1% or less of the original population, persist despite continued exposure to the antibiotic. The final stage of biofilm is dispersal, which is 2 types. Passive dispersal of biofilm which includes erosion, abrasion, sloughing causes due to fluid shear. The second type of dispersal is Active dispersal in which sessile, matrix-encased biofilm cells convert to free-swimming planktonic bacteria by the help of quorum sensing. Quorum sensing is a cell - cell signaling process in biofilm. The active dispersal is due to enzyme-mediated breakdown of the biofilm matrix, the production of surfactants which loosen cells from the biofilm, intracellular di-cyclic GMP levels, intracellular di-cyclic GMP levels and production of free radical species [5, 6, 45].

Structure of biofilm is greatly affected by detachment process. Biofilms experience continuous shear stress in aqueous medium. A 2D model biofilm detachment caused by internal stress from liquid flow is proposed by Cristian Picioreanu, et al., 2000. They observed that erosion makes relatively smoother surface than sloughing. Under same hydrodynamic condition and biofilm strength the faster growing biofilm detaches faster than slow growing biofilms. The biofilm detachment process depends on both shear and microbial growth rate. Massive sloughing can be avoided by combining high liquid shear with low biofilm growth rate. Comparatively rough surface promotes the biofilm growth in hydrodynamic condition than the smooth surface [46].

Biofilm structure is affected by both biofilm expansion (attachment of cell) and biofilm shrinking (cell detachment). The biofilm expansion is mainly due to the cell growth, which needs dissolved nutrient in liquid flow. The dissolved nutrient first passes through mass transfer boundary layer than reaches to cell by passing through biofilm matrix. Hence, the biofilm structure indirectly depends upon both diffusive and convective transport of substrate. To predict the effect of diffusive and convective transport of substrate on biofilm structure, a 2D model is proposed by Picioreanu et al., 2000. This model includes flow computation around the irregular biofilm surface, substrate mass transfer by convection and diffusion, biomass growth and biomass spreading. They observed that biofilm growth regime limited by the rate of substrate transport which resulted in rough biofilm surface. As the nutrient availability increases, the biofilm becomes smoother and compact. The

convection and flow-driving mechanism have not shown any significant role in determining biofilm structures. Smaller number of initial colonies leads to a rough biofilm structure whereas larger number of initial colonies gives a relatively a smoother surface [46].

A computational model called individual-based modelling (IbM) is use to understand the complex organization of biofilms from the interactions of its parts, individual cells and their environment. IbM is a bottom-up approach, attempts to model a population or community by describing the actions and properties of the individuals in community. IbM allows individual variability and treats organisms, as the fundamental entities. Where the characteristics of each individual (Bacteria in our case) are tracked through time. This is an improved version of biomass-based model (BbM). In both models biofilm growth occurs due the process of substrate diffusion, reaction, cell growth and spreading of cell. In the BbM, biomass was distributed in a discrete grid and each species had uniform growth parameters. Whereas IbM takes a different approach for biomass distribution. In IbM, spreading of biomass occurred by pushing of cells to minimize overlap between cells. In IbM, when cells changes their positions all the properties of cell are remains unchanged. Biofilm growth is usually a much slower process than diffusion of substrate into the biofilm. The diffusion process can be simulated assuming the growth process to be frozen, and the growth process can be simulated assuming the diffusion process to be in a pseudo-steady state, which is physically relevant. A 2D space for substrate diffusion and 3D space for biomass distribution is used. Initially number of cell placed randomly chosen locations on the surface of the substratum. A mass transfer boundary layer maintenance a constant distance form top of biofilm. The zero flux boundary condition is assumed at the substratum. At the top of the system, the bulk liquid with constant substrate concentration was located. To avoid edge effects a periodic boundary condition is applied in both sides [47]. The IbM which utilizes a griddles domain for biomass distribution, track the individuals through time which makes the model complex. Further it is weak in representing entire trophic environment and validation needed for many biological parameters.

Another model called cellular automata model (CA) is proposed by Picioreanu et al., 1997, in which space is represented by a uniform grid. The main difference between IbM and CA is, IbM utilizes a grid less domain for biomass distribution whereas CA has a uniform grid sapce for biomass distribution. In CA, Time advances in discrete steps, and at each step each grid computes its new state from that of its close neighbours. This model predict the biofilm structure by combining discrete representation of the solid phase with classical continuous methods for soluble components. Biomass distribution can achieved by cell shoving process. Step-1, when a cell divides the mother cell stays at original site whereas daughter cell search for new free space among nearest-neighbor elements. Step-2, if there are more free adjacent elements around than daughter cell is placed in one of them chosen at random. Step-3, if there are no free elements for the daughter cell then the daughter cell will displace a neighbor cell chosen at random. Step-4,The displaced cell will search again for a free-space element by same process [26]. This CA is model is applied in Dynamic modelling of cell death during biofilm development, by Fagerlind group with little modification [48]. Instead of random choice at Step-3 they have taken the neighbour cell which offers less resistance, in case if more than one neighbour cell offers same resistance than one of them chosen at random. Same process is also applied at Step-4.

A relatively advance, discrete differential modeling for biofilm structure is proposed by Picioreanu et al., 1999. Which incorporates the flow over the irregular biofilm surface, convective and diffusive

mass transport of substrate, bacterial growth and biomass distribution. In reality biofilm growth is much slower than rate of diffusion of substrate in biofilm. Also, momentum transport is much faster than diffusive mass transport. Which is taken into account in this model, by time scale analysis [27]. The objective of this study is to select a suitable model to simulate biofilm growth. A 3D CA model is selected for simulation.

Chapter 3

Methods

Modelling of biofilm development performed in a three-dimensional spatial domain using discrete-stochastic cellular automaton approach. In this article, the individual based cellular automaton model is applied to simulate initiation and growth of biofilms attached on solid flat surfaces in an aqueous environment. Microbial cells treated as independent entities with own set of parameters. Our 3D model accounts for the nutrient transport gradients, EPS, QS, liquid flow, etc. and, from this, the biofilm structure is modeled implicitly.

3.1 Biofilm simulation domain geometry

We considered a 3D rectangular geometry with dimensions $L_x * L_y * L_z$, and spatially discretized into cubic volume elements with size of each side as $3 \mu\text{m}$. In 3D Cartesian grid, coordinates of elements are given by vector $(x, y, z) \in (0 \dots X_{max} - 1, 0 \dots Y_{max} - 1, 0 \dots Z_{max} - 1)$. On the flat solid substratum at the bottom of the simulation domain, a small population of bacterial cells adhered initially at randomly chosen positions (at $Y = 0$). The bulk liquid compartment situated at the top of the geometry is the constant source of soluble substrate and allows its diffusion to biofilm compartment through mass transfer boundary layer inside a rectangular box with periodic x and z boundaries. Apart from nutrients and biomass in domain sites, biofilm compartment also contains extracellular polysaccharide, and quorum sensing molecules or equal volume of liquid. Quorum sensing molecules, substrate, microbial cells, and other material are assumed to be scraped once they reach the detachment layer (Y_{max} boundary).

Three boundary conditions have been applied to our system:

(1) In order to avoid edge affect and to maintain continuity of biofilm biomass a periodic boundary condition has been applied to both X and Z direction. For example, the periodic boundary condition implemented in the X direction means that each grid element at $X = N - 1$ has nearest neighbor element at $X = 0$ sharing the same Y and Z coordinates.

(2) An ideal planar source of substrate is placed in all computational elements situated at a certain position (At mass transfer Boundary layer), meaning that the fixed-value boundary condition (Dirichlet boundary condition) is imposed for any grid element at mass transfer boundary layer. Mass transfer boundary layer is always situated at a fixed distance above the top of the biofilm. Thus, the source of substrate will move upward in time while the biofilm grows.

(3) The zero-flux boundary condition is assumed at the solid wall on the bottom. Meaning concentration gradient at solid bottom wall is zero.

The state of the simulation geometry updated at discrete time steps, by performing the following calculations at each step in a sequential manner.

Calculating for substrate transport and diffusion reactions (equilibrium reactions).

Calculating for each bacterial cell growth based on nutrient bio conversion.

Calculating for the damage concentration of microbial cell based on its maintenance.

Checking for biomass division and spreading to describe increase in bacteria number and also EPS production.

Checking for bacterial cell death and detachment based.

Attaining equilibrium condition for autoinducer.

Checking for QS.

3.2 Substrate transport and transformation

Nutrient diffusion is performed globally over all discretized elements. The substrate concentration in biofilm compartment depends on the balance between substrate transport mechanism due to diffusion and substrate transformation rate in the microbial cells. Also it is clearly shown that flow around microbial mat influences the transport of solutes, production of exopolysaccharides, and metabolic/genetic behaviors of biofilms [5, 46, 48, 49].

We modeled nutrient transport and transformation with in each site of geometry by using a discretized form of the three-dimensional diffusion-reaction-convection equation.

$$\frac{\partial S_c}{\partial t} = D_s \left(\frac{\partial^2 S_c}{\partial x^2} + \frac{\partial^2 S_c}{\partial y^2} + \frac{\partial^2 S_c}{\partial z^2} \right) - r_s(S_c, B_c) - \nabla \cdot (vS_c) \quad (3.1)$$

Here $S_c = S_{c_{x,y,z,t}}$ and $B_c = B_{c_{x,y,z,t}}$ represents the substrate and biomass concentration with in each spatial element x,y,z at every time step t , respectively. While the convective term used to bulk substrate transport. Initially, substrate concentration at all elements of the lattice is zero, except for those present in the bulk liquid reservoir, where the substrate concentration assumed maximum, S_{SB} . D_s is the substrate diffusion constant and r_s is the reaction term corresponding to the substrate consumption by the bacteria. The diffusivity in the biolm is determined by multiplying the diffusion rate of nutrients in the aqueous or bulk phase, $D_{S,aq}$, by the relative effective diffusivity, $D_{S,e}/D_{S,aq}$.

Nutrient consumption by the bacteria depends on the substrate concentration, S_c and the biomass concentration, B_c in biofilm. The rate term, usually expressed as a classical Monod like saturation function:

$$r_s(S_c, B_c) = \left(\frac{\mu_{max}}{Y_{SB}} + m_s \right) B_c \frac{S_c}{K_s + S_c} \quad (3.2)$$

Here μ_{max} denotes the maximum specific growth rate of cells, Y_{SB} is the cell growth yield from substrate, m_s is the maintenance coefficient and denotes the half saturation constant.

3.3 Rate of biomass production

Biomass production kinetics is dependent on nutrients availability and endogenous metabolic pathways involved in their maintenance. Biomass concentration of a single bacterial cell entity is varying with time via two mechanisms:

(i) Increases due to nutrient consumption, and

(ii) Decreases due to nutrient consumption for own metabolic processes; the rate of decrease of biomass by the second mechanism assumed to be directly proportional to the biomass concentration [48, 50, 51]. Furthermore, the unconsumed nutrient will be converted to biomass based on a pre-determined efficiency parameter, the yield coefficient (Y_{SB}). The net rate of biomass formation in each cell computed by considering substrate consumption rate term and its maintenance requirements:

$$\frac{\partial B_c}{\partial t} = Y_{SB} (r_s(S_c, B_c) - mB_c) \quad (3.3)$$

3.4 Cell division

Biomass spreading and biofilm detachment generates the heterogeneity in self-organized biofilm morphological characteristics. In our model we used an improved approach for biomass redistribution known as path of least resistance. Bacterial cells will continue to grow and divide within a grid location due to adequate nutrients. Once the biomass content in the grid element in which it has grown above the maximum biomass density (V_d), it elongates and pinch off into two equal parts, i.e. two daughter cells from single parent cell. As biomass is growing, newly generated cells have to be reallocated in empty grid elements available in biofilm compartment. One daughter cell stays remains in the original location and the other daughter cell make free space adjacent to mother cell location by pushing neighbors in the direction of shortest distance [51, 52].

After bacterial cell division step, one of the two new cells checks for empty space around the original location in all possible 26 directions (1 for each of the 6 faces, 12 edges and 8 vertices of the cube). If all the 26 elements around the parent elements are occupied with biomass, then computational algorithm allows the bacterial cell to identify free space at increasing distance from the overfilled compartment. The first available empty site will be occupied by new cell by displacing the entire row or column or a combination of rows and columns of cells between the dividing cell and closest free space. If there are two or more directions with equal distance having unoccupied elements, one of is chosen at random choice. This process repeats until an empty site is located with minimal resistance to make free space in chosen direction. Thus, when a cell which is embedded deep within the microbial mat divides, nearby solid entities such as active biomass effectively pushes out of the way to make space for new cells in the lattice cube and extend the biofilm structure [5, 53].

3.5 Cell death

Recent studies have revealed that regulated (programmed cell death or apoptosis) autolysis of bacterial cells and cell death in deep of the biofilm play important role in intercellular adhesion and biofilm structural stability [17, 18]. Various endogenous metabolic pathways present in the bacterial

species helps to increase rate of biomass production and manage their maintenance by substrate consumption at a fixed efficiency given by the yield coefficient [48]. A dead cell is a cell that no longer consumes substrate and divides, is removed from the simulation entity and leaves a free space in biofilm. Eventually near by dividing daughter cells can occupy the empty elements left behind by dead or lysed cells. Microbial cell maintenance under minimal nutrient concentrations leads to cell shrinkage and serves as energy reserve for neighboring population. In our biofilm development simulation death of aged colony counter is estimated by availing user-controllable parameter R , which is the ratio between biomass formation and endogenous metabolism. Bacteria yields net growth if R is higher than 1 else biomass falls below a minimum value and cell has reached stationary phase.

Cellular automata rules for bacterial cell death:

(1) Bacteria die if they have been in stationary phase for a specific number of hours (N_H). This is recorded with an individual based counter. If R is below 1 during one hour, the counter increases by one. However, a bacterium also has the possibility to recover if R increases above 1 before it dies. Consequently, if R is above 1 during one hour, the counter decreases by one. However, the counter can never be less than zero.

(2) Bacteria die if R falls below a certain threshold value. This is an attempt to account for bacterial death under circumstances of low (or no) substrate concentration.

3.6 Cell detachment

Biofilm dispersal is the crucial stage of biofilm cycle due to its contribution to the dissemination of contamination and infection in both clinical and public health settings. Disease transmission due to biofilm cell detachment is a complex process which includes three different phases such as bacterial cell detachment from microbial mat, translocation of detached bacterial cell to the new site, and regrowth cells and development of biofilm after reattachment of the dispersed cells at the new location. Detachment of biomass from bacterial biofilms, based on the magnitude and frequency of the detachment event may range from single cell or small portions of the clusters with a diameter of approximately $500 \mu\text{m}$ to massive loss of biofilms, known as erosion and sloughing respectively [41, 54, 55]. The detachment and dispersal of bacterial cells from biofilm colony in to the surrounding environment is the last stage of biofilm development involves various environmental signals and effectors, and signal transduction pathways. Detachment of cell occurs, if cell loses contact with primary biofilm mass due to cell death.

3.7 EPS Production

Extracellular polymeric substances (EPS) is the abode of microbial cells which represent the conditions prevalent in the immediate environment in which cells reside by affecting various factors such as porosity, water content, sorption properties, mass transport, and mechanical stability [13, 25, 56, 57]. Even though EPS matrix present as a barrier between bacterium and its surrounding environment, it contributes various functions such as bacterial adherence to surfaces and neighboring cells, enhance nutrient capture, and resistance to host environmental stress and antibiotic and disinfectant agents [58]. The biopolymer represent the house of the biofilm cells, if the virulent biofilm can be called as a city of microbes [59]. Most of biofilm associated infectious diseases in the host

system are very difficult to diagnose efficiently due to lack of knowledge necessary to find out exact precursor which facilitate the complexity of sessile community. Kreft et. al., have simulated mixed-species biofilm using 3D individual based model in order to elucidate the effect of various extracellular polymeric substance (EPS) production scenarios on biofilm structure and function. Their observations explained that, EPS production decreased growth of producers and stimulated growth of non-producers because of the energy cost involved. The patchiness and roughness of the biofilm decreased and the porosity increased due to EPS production [50]. Jin Xiao et.al. Explored the mechanisms through which the *Streptococcus* mutants-produced EPS-matrix modulates the three-dimensional (3D) architecture and the population shifts during morphogenesis of biofilms on a saliva-coated-apatitic surface using a mixed-bacterial species system [60].

Once the EPS volume in given grid element exceeds threshold value, it divides in to two parts and 50% eps move to new element by path of least resistance protocol. The EPS matrix is described by a continuum representation as incompressible viscous fluid, which can expand and retract due to generation and consumption processes. The cells move due to a pushing mechanism between cells in colonies and by an advective mechanism supported by the EPS dynamics. Detachment of both cells and EPS follows a continuum approach, whereas cells attach in discrete events. The net rate of EPS formation by every bacterial cell was computed by considering substrate consumption rate and cell maintenance requirements:

$$\frac{\partial E_c}{\partial t} = Y_{SE} (r_s(S_c, B_c) - mB_c) \quad (3.4)$$

Where Y_{SE} yield coefficient of EPS production.

3.8 Quorum sensing

Microbial cell present in self-enclosed matrix communicate with its neighboring cells to coordinate their behavior and functions by a chemical signaling process referred as quorum sensing. The chemical communication process in biofilm development triggered after bacterial cell response towards a small hormone-like molecules known as autoinducers (AI). A diverse array of diffusible extracellular molecules (AIs) mediates bacterial cell to cell signaling pathway and facilitate critical intra-and-inter species relationships. The accumulation a stimulatory concentration of an extracellular autoinducers in the environment increases effectively in response to changes in the number of cells present in bacterial community [61, 62]. Using this signal-response system, bacteria collectively alter gene expression and behavior in response to minimal threshold concentration of signaling molecules present in microenvironment like positive feedback loop. In general, the cyclic-peptide-dependent accessory gene regulator (*agr*) quorum-sensing system in *Staphylococcus aureus* represses several surface adhesins that mediate contact with the host matrix. Under certain conditions, *agr* mutants adhere more efficiently than wild-type strains to both biological and abiotic surfaces [63, 64, 65]. *P. aeruginosa* uses extracellular quorum-sensing signals (extracellular chemical signals that cue cell-density-dependent gene expression) to coordinate colonization in lungs causes cystic fibrosis [37].

Microbial cell present in each element switch between up-regulated and down-regulated states as the concentration of autoinducer or inhibitor changes respectively [61]. In the presence of inhibitor,

the transition rate from down-regulated to up-regulated states is taken to be

$$Q^+ = \alpha \frac{A_c}{1 + \gamma(A_c + \bar{A}_c)} \quad (3.5)$$

Where A_c and \bar{A}_c are concentration of autoinducer and inhibitor respectively Where α and γ are constants. The probability of a cell changing from down- to up-regulated is given by

$$P_{up} = Q^+ \Delta t \quad (3.6)$$

The transition rate from up-regulated to down-regulated states is taken to be

$$Q^- = \beta \frac{1 + \gamma \bar{A}_c}{1 + \gamma(A_c + \bar{A}_c)} \quad (3.7)$$

Where β and γ are constants. The probability of a cell changing from up- to down-regulated is given by

$$P_{down} = Q^- \Delta t \quad (3.8)$$

3.9 Autoinducer transport and transformation

Its autoinducer concentration which determines whether a cell to be up-regulate or down-regulate. We assumed that the concentration of autoinducer in the bulk liquid is zero. Production of autoinducer by the cell depends upon whether the cell is up-regulated or down-regulated. As similar to substrate concentration calculation also used to calculate autoinducer concentration.

$$\frac{\partial A_c}{\partial t} = D_A \left(\frac{\partial^2 A_c}{\partial x^2} + \frac{\partial^2 A_c}{\partial y^2} + \frac{\partial^2 A_c}{\partial z^2} \right) + \frac{F}{L^3} - \nabla \cdot (v A_c) \quad (3.9)$$

where, $F = Z_{A,u}$ for up regulated cells and $Z_{A,d}$ for down regulated cells

3.10 Antimicrobial drug administration and killing

Most of the times antibiotics are not effective against organisms in biofilm-associated infections. The main cause of reduced susceptibility of microcolonies and biofilm towards antibiotic therapies lies within the extensive or repeated use of nonspecific antimicrobial agents to control chronic infections. Modern science is receiving challenges in bacterial biofilm diagnosis and to explain how cells in biofilm promoting increased tolerance to host defenses and antibacterial agents, unlike planktonic cells. In this study, we demonstrate biofilm dynamics using a cellular automaton model which allows to develop *Pseudomonas aeruginosa* biofilm with realistic structural heterogeneity and emulate physiology mechanisms of bacterial cells in biofilm resistance to antimicrobial agents. Our work introduce a computational model as a tool to predict the cell death and cell detachment phenomenon during antimicrobial drug administration. Microbial cell detachment is an important process that destabilizes and disrupts the biofilm architecture and it is a critical determinant of the dynamics of biomass accumulation and loss.

We modeled antibiotic drug transport and transformation with in each square of the geometry

by using a discretized form of the three-dimensional diffusion-reaction-convection equation.

$$\frac{\partial C_{Ab}}{\partial t} = D_{Ab} \left(\frac{\partial^2 C_{Ab}}{\partial x^2} + \frac{\partial^2 C_{Ab}}{\partial y^2} + \frac{\partial^2 C_{Ab}}{\partial z^2} \right) - r_{Ab}(C_{Ab}, B_c) - \nabla \cdot (v C_{Ab}) \quad (3.10)$$

Here C_{Ab} and B_c represents antibiotic and biomass concentration with in each spatial element x, y, z at every time step t , respectively. While the convective term used to bulk transport of drug. Initially, antimicrobial agent concentration at all elements of the lattice is zero, except for those present in the bulk liquid reservoir, where its concentration assumed maximum. D_{Ab} is the antibiotic diffusion constant and r_{Ab} is the reaction term corresponding to the antibiotic consumption by the bacteria. The rate term expresses as:

$$r_{Ab}(C_{Ab}, B_c) = K_{A_{max}} B_c \frac{C_{Ab}}{K_{Ab} + C_{Ab}} \quad (3.11)$$

Where, $K_{A_{max}}$ represents Maximum specific reaction rate of antibiotic and K_{Ab} is Half saturation coefficient of antibiotic.

The probability of cell death due to antibiotic consumption is given by:

$$P = \frac{r_{Ab} - r_{BIC}}{r_{max} - r_{BIC}} \quad (3.12)$$

Where, r_{Ab} is rate of consumption of antibiotic, r_{BIC} is rate of consumption of antibiotic at biofilm inhibitory concentration and r_{max} is the Maximum antibiotic consumption rate. Cell dies if the generated random number is less than probability of killing.

Cogan et. al. Presented a mathematical model to study the pulsed dosing antimicrobial agents action on bacterial biofilms. Their 2-dimensional model included the fluid dynamics in and around the biofilm, advective and diffusive transport of two chemical constituents and the mechanism of physiological resistance. The final survival fraction for longer exposure is two orders of magnitude less than that of the shortest dose duration, indicating, exposing the biofilm to low concentration doses of antimicrobial agent for longer time is more effective than short time dosing with high antimicrobial agent concentration [66].

Table 3.1: Definition of variables and parameters

Parameter/Variable	Description	Values	Unit
μ_{max}	Maximum specific growth rate	0.3125	h^{-1}
Δt	Time step used for CA	1	h
Δl	The element size	3×10^{-6}	m
B_{LT}	Thickness of the mass transfer boundary layer	18×10^{-6}	m
B_c	Biomass concentration		$gm\ m^{-3}$
D_s	Diffusion coefficient of substrate		$m^2\ h^{-1}$
$D_{s,aq}$	Diffusion coefficient of substrate (glucose) in the aqueous phase		$m^2\ h^{-1}$
$D_{s,e}/D_{s,aq}$	Relative effective diffusivity of substrate in the biolm	1/3	Unitless
E_x	Number of elements in x-direction	40	Unitless
E_z	Number of elements in z-direction	40	Unitless
K_s	Half-saturation coefficient of substrate	2.55	$gm\ m^{-3}$
m	Maintenance coefficient	0.036	$g_s g_b h^{-1}$
N_H	Number of hours in stationary phase at which cell death occur	24-108	Unitless
S_{SB}	Substrate concentration in bulk phase	3,5	$gm\ m^{-3}$
S_c	Substrate concentration		$gm\ m^{-3}$
Y_{SB}	Yield coefficient of biomass production	0.45	$g_b g_s^{-1}$
Y_{SE}	Yield coefficient of EPS production	0.289	$g_e g_s^{-1}$
$\overline{A_c}$	Inhibitor concentration	0	$gm\ m^{-3}$
A_c	Autoinducer concentration		$gm\ m^{-3}$
$Z_{A,u}$	Autoinducer production by up regulated cells	73800	molecules m^{-3}
$Z_{A,d}$	Autoinducer production by down regulated cells	498	molecules m^{-3}
β	Spontaneous down regulation rate	0.975	h^{-1}
α	Conversion rate for Up regulation	7.89×10^{-17}	h^{-1}
γ	Transition rate constant	7.95×10^{-17}	$m^3\ molecules$
K_A	half saturation coefficient of antibiotic	1	$gm\ m^{-3}$
$K_{A_{max}}$	Maximum specific reaction rate of anitibiotic	2.5	h^{-1}
V_d	Biomass Division Value	2×10^{-12}	gm
E_d	EPS Division Value	33000	$gm\ m^{-3}$

Chapter 4

Results and Discussions

A cellular automata model has been used to investigate the effect of antimicrobial agents on *Pseudomonas aeruginosa* biofilm growth and its susceptibility, where microbial population were exposed to an antibiotic for 48 continuous simulation hours. Initially we started our computational simulations of *Pseudomonas aeruginosa* biofilm development and evaluated the structural properties under two nutrient substrate concentrations 3gm m^{-3} , and 5gm m^{-3} without antimicrobial therapy. Due to stochastic nature of the model, individual results of simulated biofilms experiments were never exactly copied, even though simulations were ran under similar parameters. Since it is not possible to present all of the simulation results, here we are presenting few of selected. In order to obtain biofilm structure, biomass concentrations were plotted using MATLAB at different time steps for two substrate concentrations. Initially bacterial population goes into an exponential phase where biofilm develops very fast with time, followed by an oscillating stationary phase where the cell density does not varies much, and shadowed by cell detachment process. The bacteria assumed to be dead if it presents in stationary phase for a given period of hours (N_H) or if the local nutrient concentration goes below a certain threshold value. During the biofilm development simulation, we fixed the number of stationary hours at which cell dies (N_H) is 24h. We found that primary cell death occurs at the bottom of the biofilm, which is due to the fact that continuous nutritional depletion at the bottom of the biofilm 4.1 and 4.2.

With higher nutrient concentration bacterial cells can generate a faster growing biofilm. Due to high cell density, they consume huge amount of substrate which leads to a steeper nutrient gradient in microbial mat. Cells which are in interior part of the biofilm goes into continuous starvation due to no or very less availability of nutrient, leads to early cell death and causes high damage to the biofilm 4.3 .

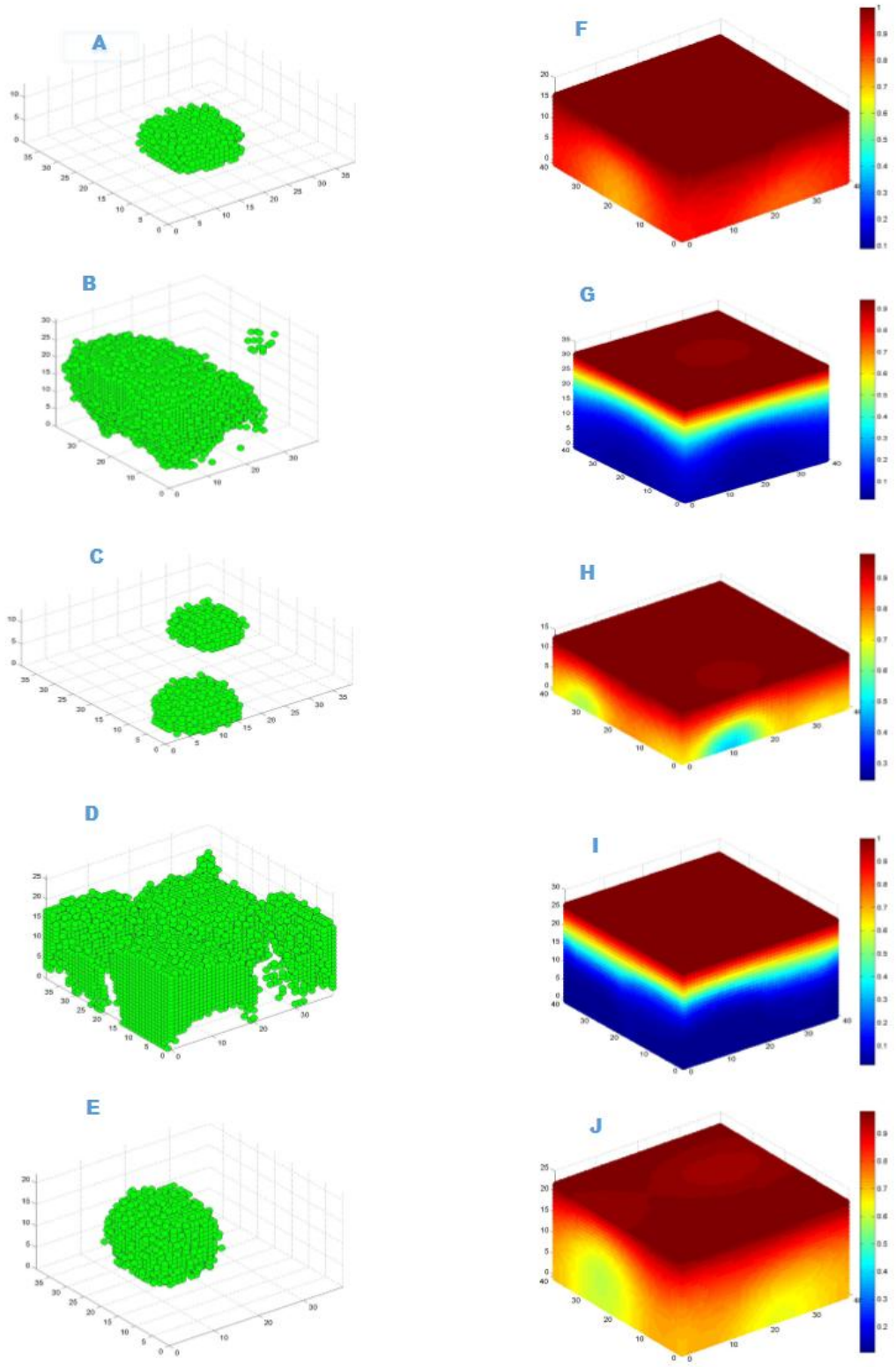


Figure 4.1: The plot showing a simulation results in which bacteria, growing with bulk phase concentration S_{SB} of 3 gs m⁻³ and respective substrate profiles in our simulation domain at different time steps, A) 50 hr., B) 130 hr., C) 200 hr., D) 270 hr., and E) 400 hr.. The colour scale represents the substrate concentration in our computational domain.

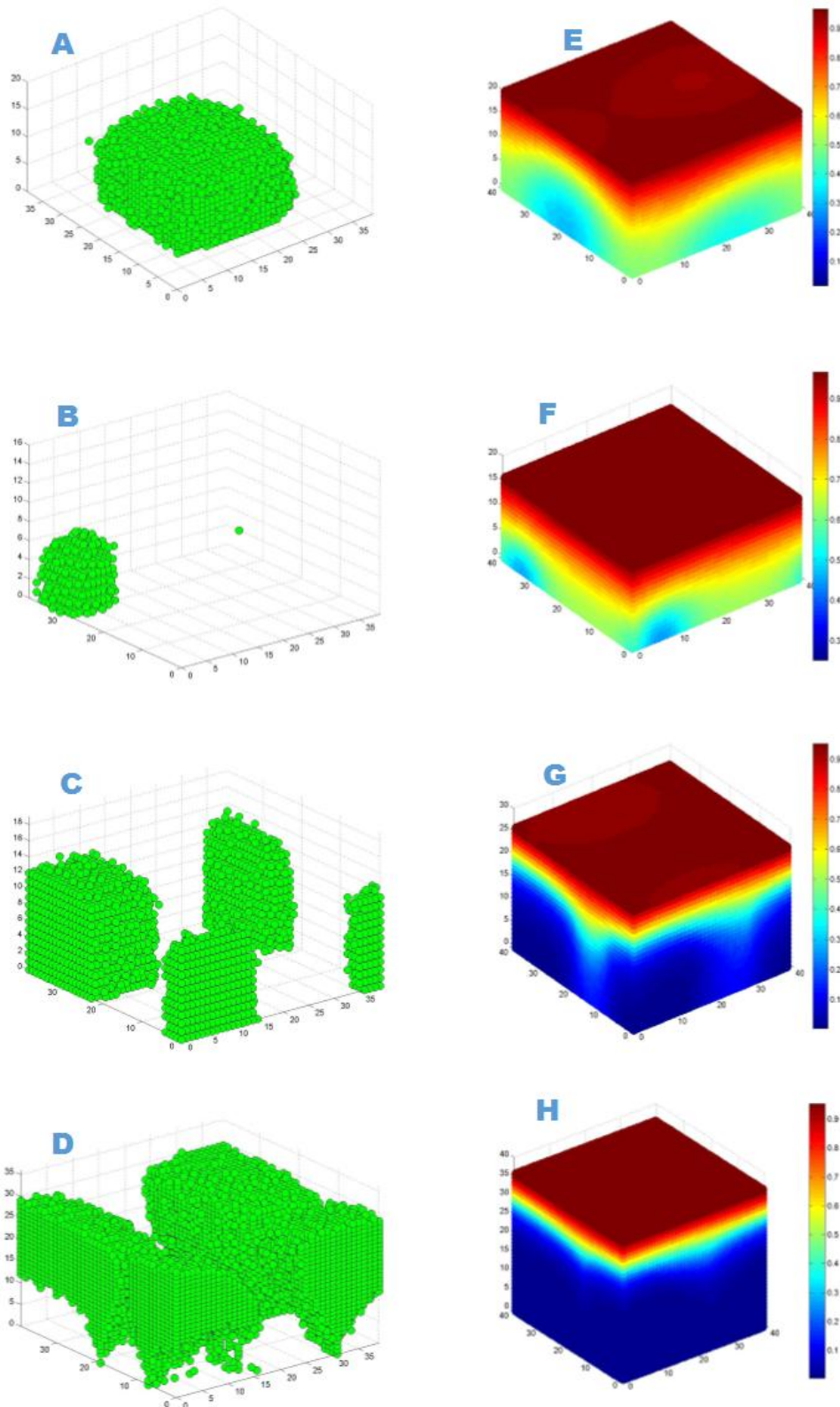


Figure 4.2: The plot showing a simulation results in which bacteria, growing with bulk phase concentration S_{SB} of 5 gs m⁻³ and respective substrate profiles in our simulation domain at different time steps, A) 50 hr., B) 130 hr., C) 200 hr., D) 270 hr., and E) 400 hr.. The colour scale represents the substrate concentration in our computational domain

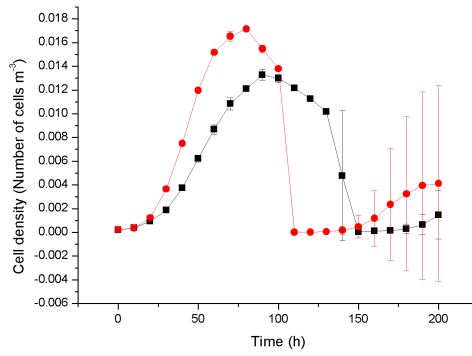


Figure 4.3: The plot showing the *Pseudomonas aeruginosa* biofilm cell density during biofilm development at two different substrate concentrations 3gm m⁻³ (Square symbol), and 5 gm m⁻³ (Round symbol), as a function of time (0 – 200 hrs.) without antimicrobial therapy. *Time series of fraction of biofilm detached data representing mean and standard deviation from four replicate simulations.

During biofilm development cell lysis happens due to substrate depletion which leaves hallowed interior biofilm, leads to loosely connected biofilm to the substratum. Then bacterial cells which anchor as the large chunk can expect to be detached due to nutrient starvation. Probably detachment provides a mechanism for cells to migrate from heavily colonized areas that have been depleted of surface-adsorbed nutrients to areas more supportive of growth and form secondary colonies. Cells can be connected to biofilm through attached cells in surrounding or through EPS matrix. Biofilm cell viability, compactness, and detachment process will depend on growth behaviour of microbial cells. We approached a simple rule for detachment event that, when a cell loses its connection from the primary biofilm it detaches, by assuming bulk fluid forces doesnt affect the detachment process. The detachment event varies from simulation to simulation because it depends upon the number of cell died and also their position. Bacterial population density depends upon the growth conditions and survival of daughter cells. In favourable condition bacterial cells adapt easily and grow faster. To observe this phenomenon we ran few simulations with varying substrate concentration. In higher substrate concentration bacteria grows faster which gives higher cell population compared to lower substrate concentration. In other hand cell population dramatically decreases due to microbial detachment which observed in between 100 – 170h 4.4.

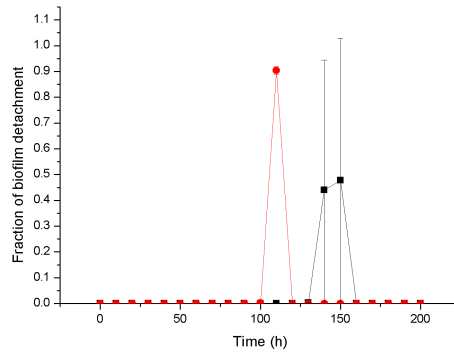


Figure 4.4: The plot showing the variation of *Pseudomonas aeruginosa* biofilm detachment during microbial mat development at two different substrate concentrations 3gm m-3 (Square symbol), and 5 gm m-3(Round symbol), as a function of time (0 – 200 hrs.) without antimicrobial therapy. *Time series of fraction of biofilm detached data representing mean and standard deviation from four replicate simulations.

Special structural organization of the biofilm brings individual cell into a very intact form, helps biofilm to resist compounds like antibiotic and also in exchanging of genetic material in between cells of the biofilm. Adjacent placement of inoculum during computational biofilm simulation forms a high compact structure initially. Cells growing slowly in biofilm remains anchored and compact form for extended duration, whereas cells with rapid growth rate are unlike 4.5.

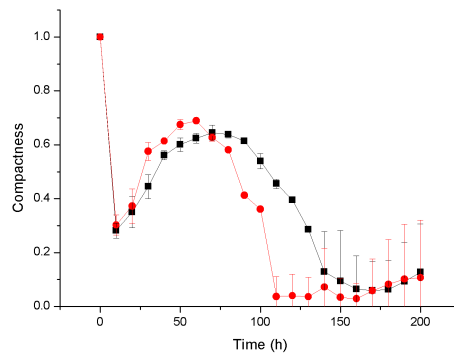


Figure 4.5: The plot showing the variation of *Pseudomonas aeruginosa* biofilm compactness during microbial growth at two different substrate concentrations 3gm m-3 (Square symbol), and 5 gm m-3(Round symbol), as a function of time (0 – 200 hrs.) without antimicrobial therapy. *Time series of fraction of biofilm detached data representing mean and standard deviation from four replicate simulations.

Cell viability fraction is calculated to trace the viable cells present in biofilms under various two substrate concentrations. While cells growing faster in higher substrate concentration leads to quick cell death phenomenon and causes early viable cell fraction reduction, whereas slow growing cells in low substrate concentration retains viable for prolonged time 4.6.

Biofilm surface roughness is defined as the ratio between standard deviation of the height of the biofilm to its mean height. Surface roughness is one of the factors having significant impact on

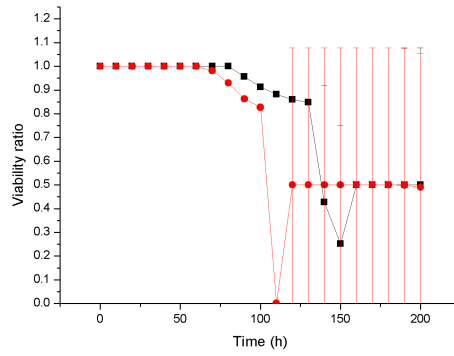


Figure 4.6: The plot showing the cell viability ratio of *Pseudomonas aeruginosa* cells during biofilm development at different substrate concentrations 3gm m⁻³ (Square symbol), and 5 gm m⁻³ (Round symbol), as a function of time (0 – 200 hrs.) without antimicrobial therapy. *Time series of fraction of biofilm detached data representing mean and standard deviation from four replicate simulations.

the thickness of the biofilm boundary layer over which bulk fluid travels. Rough biofilms facilitate boundary layer mass transport to biofilms and improve rate of nutrient diffusion into biofilms. Consequently improved mass transfer of nutrients to microbial population will result in cell growth rate augmentation, which also may be one of the reasons for having higher cell population in higher substrate concentration. At high substrate concentration due to early detachment, biofilm shows relatively rougher surface compare to low substrate concentration 4.7.

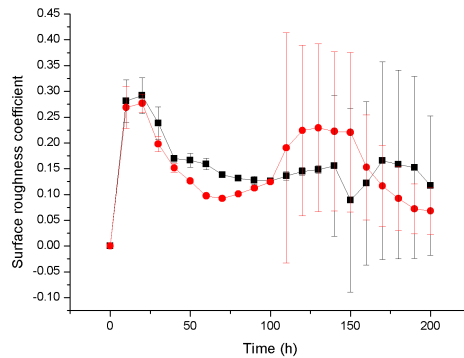


Figure 4.7: The plot showing the *Pseudomonas aeruginosa* biofilm surface roughness during biofilm development at two different substrate concentrations 3gm m⁻³ (Square symbol), and 5 gm m⁻³ (Round symbol), as a function of time (0 – 200 hrs.) without antimicrobial therapy. *Time series of fraction of biofilm detached data representing mean and standard deviation from four replicate simulations.

4.1 Antibiotic concentration dependent Biofilm resistance

There are different mechanisms of antibiotic resistance of bacterial population in biofilm mode of growth have been reported such as, depletion of antimicrobial agents by reaction with biomass or physiological resistance due to reduced bacterial growth in the biofilm [67]. To investigate antibiotic concentration dependent killing, *Pseudomonas aeruginosa* biofilms were grown in 3gm m^{-3} nutrient concentration with various antimicrobial concentrations. Antibiotic agent concentration was varied from 0 gm^{-3} to 10 gm^{-3} to observe *Pseudomonas aeruginosa* biofilms susceptibility. Antimicrobial therapy was initiated at 40th hour of biofilm simulation and continued for next 48 hours. *Pseudomonas aeruginosa* produces β -lactamase which degrades β -lactam antibiotics and increases resistivity to antibiotic agents [68]. The diffusible antibiotic agent diffuses from the bulk fluid and reaches to the biofilm through mass transfer boundary layer and neutralized by reacting with biofilm. The neutralization process depends upon the local concentration of the antibiotic and also local biomass concentration.

The cell death caused by the antibiotic is stochastic in nature and also depends upon the neutralization reaction by the cell. In other words the cell which is exposed to high concentration of antibiotic is more prone to die. Upon antibiotic treatment, cell death starts at the surface of the biofilm where the antibiotic concentration is relatively high 4.8.

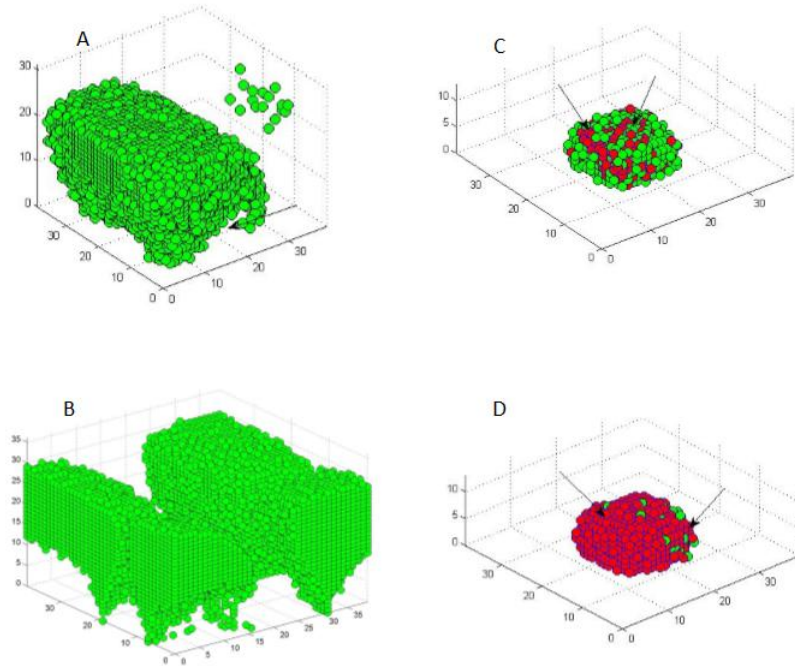


Figure 4.8: In this figure, plot A) and B) shows cell death happens at the bottom of untreated biofilm which leave a hollow structures, plot C) and D) shows antibiotic treated biofilm where most of the cell death (Red colour) happens at surface of the biofilm.

Due to penetration limitations of the antimicrobial agents through compact biofilm, slow growing cells survive at bottom core of the biofilm. The biofilms which were treated with highest concentration of antibiotic agent 10 gm m^{-3} , cell density dramatically decreases due to cell death and consequently death of whole biofilm occurs. While biofilms treated with relatively low concentration of antibiotic 5 gm m^{-3} , cells not only resist towards exposed antibiotic but also relatively extends whole biofilm life cycle compared with untreated biofilms, which was not expected 4.9.

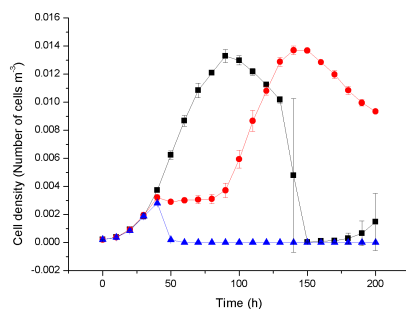


Figure 4.9: Effect of antimicrobial treatment on *Pseudomonas aeruginosa* biofilm development: plot showing cell density of *Pseudomonas aeruginosa* biofilms varied for different antibiotic agent concentrations 0 gm m^{-3} (Square symbol), 5 gmm^{-3} (Round box symbol), and 10 gm m^{-3} (Triangle symbol), as a function of time (0 200 hrs.). * Time series of the cell density data representing mean and standard deviation from four replicate simulations.

High cell population in untreated biofilms consumes a large amount of substrate as a result of which very less or no substrate presents at bottom of the biofilm, cell at the bottom goes in continuous starvation and dies. Cell death at bottom of biofilm in untreated biofilm, removes a large portion of biofilm by detachment whereas in treated biofilm the most of the cell death happens at surface of the biofilm 4.10.

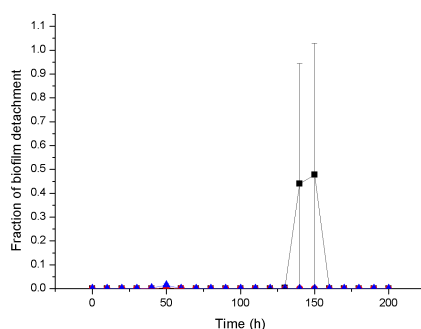


Figure 4.10: Effect of antimicrobial treatment on *Pseudomonas aeruginosa* biofilm development: plot showing the fraction of *Pseudomonas aeruginosa* biofilm detachment varied for different antibiotic agent concentrations 0 gm m^{-3} (Square symbol), 5 gmm^{-3} (Round box symbol), and 10 gm m^{-3} (Triangle symbol), as a function of time (0 200 hrs.). * Time series of the cell density data representing mean and standard deviation from four replicate simulations.

Our biofilm simulations started initially by placing 9 microbial cells in adjacent compartments at the bottom of the modelling domain, leads to form a very compact structure and structural vari-

ations were observed during microbial mat development. During 48 hrs of antimicrobial treatment of *Pseudomonas aeruginosa* biofilm, at high concentration of antibiotic 10 gm m^{-3} compactness of biofilm matrix raises and suddenly goes down due to rapid cell death happened because of antibacterial agent exposure. But biofilm simulated with similar mathematical approach treated with low concentration of antibiotic forms a very intact structure. This physiological structure may helped biofilms to resist antibiotic penetration to the bottom core of the biofilm and supported for bacterial population recovery which also clearly correlated with cell viability ratio of biofilm which is treated with low concentration of antibiotic for same duration 4.11.

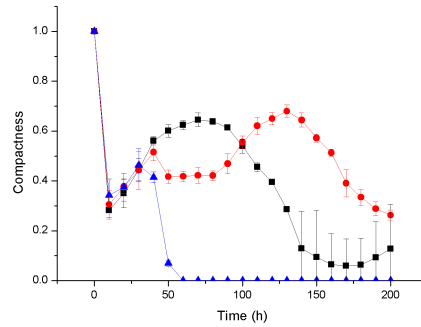


Figure 4.11: Effect of antimicrobial treatment on *Pseudomonas aeruginosa* biofilm development: plot showing compactness of *Pseudomonas aeruginosa* biofilms varied for different antibiotic agent concentrations 0 gm m^{-3} (Square symbol), 5 gmm^{-3} (Round box symbol), and 10 gm m^{-3} (Triangle symbol), as a function of time (0 200 hrs.). * Time series of the cell density data representing mean and standard deviation from four replicate simulations.

Due to sudden death, cell viability ratio of biofilm goes down continuously to zero in high concentration of antibiotic treatment. In opposite biofilm treated with minimal concentration of antimicrobial agent, microbes recover their viability ratio after few simulation hours 4.12.

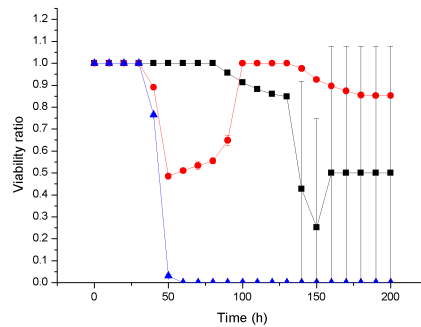


Figure 4.12: Effect of antimicrobial treatment on *Pseudomonas aeruginosa* biofilm development: plot showing the cell viability ratio *Pseudomonas aeruginosa* biofilms varied for different antibiotic agent concentrations 0 gm m^{-3} (Square symbol), 5 gmm^{-3} (Round box symbol), and 10 gm m^{-3} (Triangle symbol), as a function of time (0 200 hrs.). * Time series of the cell density data representing mean and standard deviation from four replicate simulations.

Due to continuous erosion of bacterial cells from the biofilm surface forms more rough surface

at high concentration of antibiotic treatments, whereas relatively smoother surface was observed for biofilms which were treated with low concentration of antimicrobial agents 4.13.

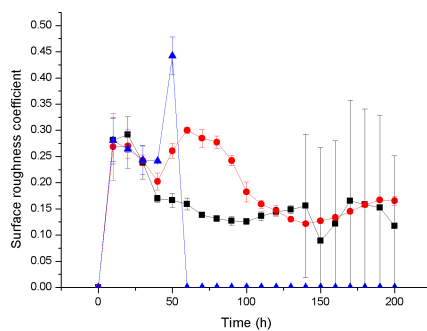


Figure 4.13: ffect of antimicrobial treatment on *Pseudomonas aeruginosa* biofilm development: plot showing the microbial mat surface roughness *Pseudomonas aeruginosa* biofilms varied for different antibiotic agent concentrations 0 gm m⁻³ (Square symbol), 5 gmm⁻³ (Round box symbol), and 10 gm m⁻³ (Triangle symbol), as a function of time (0 200 hrs.). * Time series of the cell density data representing mean and standard deviation from four replicate simulations.

4.2 Growth rate dependent Biofilm resistance

To investigate bacterial growth rate effect on biofilm resistance towards antibiotics, we varied our supplied nutrient concentration such as 3gm m^{-3} and 5gm m^{-3} and kept all other parameters as consistent. In both 3gm m^{-3} and 5gm m^{-3} nutrient concentration, antibiotic therapy was initiated after 40h of simulated biofilm growth and continued for next 48 hours with the antibiotic concentration of 10gm m^{-3} . In higher nutrient concentration the growth rate is high as a result of which cell grows relatively faster and forms a dense biomass compartment. This dense biomass compartment collectively resists the antibiotic and prevents its penetration into the biofilm. When these biofilms were treated with antibiotic agent, they entered to a stationary phase where number of cell dies due to antibiotic therapy almost equal to the number of cells generated in biofilm. After 48h of antibiotic treatment again biofilm goes into log phase and cell density dramatically changes. But when same biofilms grown at low nutrient concentration biofilm was unable to resist antibiotic and sudden death of biofilm occurs due to low growth rate 4.14.

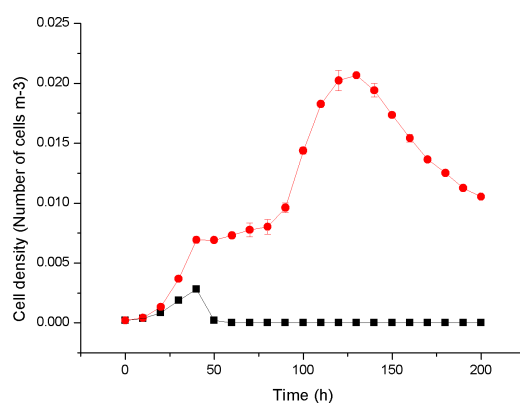


Figure 4.14: Effect of antimicrobial treatment on *Pseudomonas aeruginosa* biofilm development: plot showing cells density of the *Pseudomonas aeruginosa* biofilms varied for two different nutrient concentrations 3 gm m^{-3} (square symbol), and 5 gm m^{-3} (round symbol), as a function of time (0 200 hrs.).

Due to high number of cell the biofilm grown under high substrate concentration forms a compact structure. Due to high compactness of the biofilm antimicrobial agents unable to penetrate to the core bottom of the biofilm as a result of which biofilm resist higher concentration of antibiotic also 4.15.

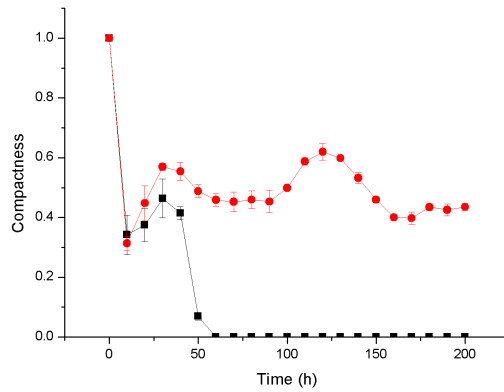


Figure 4.15: Effect of antimicrobial treatment on *Pseudomonas aeruginosa* biofilm development: plot showing the compactness of the *Pseudomonas aeruginosa* biofilms varied for two different nutrient concentrations 3 gm m⁻³ (square symbol), and 5 gm m⁻³(round symbol), as a function of time (0 200 hrs.).

Similarly cell viability ratio in high growth rate at high substrate concentration goes down at the starting of the antibiotic therapy and remains constant during treatment whereas viability ratio the biofilm having low growth rate at lower substrate concentration goes down to zero due to high susceptibility 4.16.

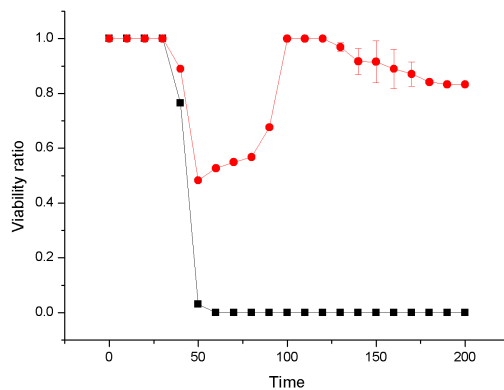


Figure 4.16: Effect of antimicrobial treatment on *Pseudomonas aeruginosa* biofilm development: plot showing the cell viability ratio of the *Pseudomonas aeruginosa* biofilms varied for two different nutrient concentrations 3 gm m⁻³ (square symbol), and 5 gm m⁻³(round symbol), as a function of time (0 200 hrs.).

Antibiotic therapy causes a high damage to slow growing biofilm and demolishes the biofilm structure as a result of which a rougher surface forms whereas faster growing biofilm continuous generates cells which fills the gap of the biofilms and makes it smoother 4.17.

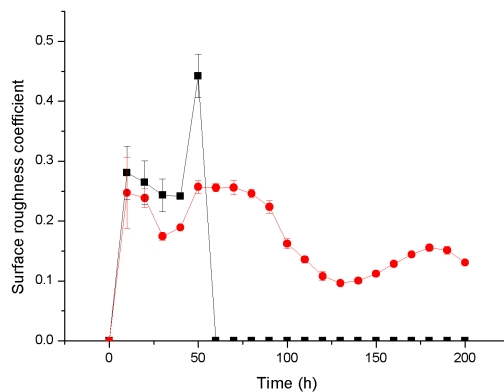


Figure 4.17: Effect of antimicrobial treatment on *Pseudomonas aeruginosa* biofilm development: plot showing the microbial mat surface roughness of the *Pseudomonas aeruginosa* biofilms varied for two different nutrient concentrations 3 gm m⁻³ (square symbol), and 5 gm m⁻³(round symbol), as a function of time (0 200 hrs.).

Chapter 5

Conclusion

A 3D cellular automata model has been developed as a tool to explain/investigate antibiotic susceptibility of biofilm. Our investigation shows that faster growing cells dies faster and cell death starts at bottom of the untreated biofilms due to continuous nutritional depletion. While treating the biofilm with low concentration of antibiotic, faster growing biofilms forms a very compact structure which may help to ripple the antimicrobial agents from the biofilm and shows complete resistance to antimicrobial agents. Likewise antimicrobial therapy at low concentration may allow regrowth of the biofilm by killing cells at the top of the biofilm which probably leads to the substrate penetration to the bottom of the biofilm. At high concentration of antibiotic treatment, structure of the biofilm disturbs and form a rougher surface due to bacterial cell erosion from surface. We observed that resistance of the biofilm not only depends on the concentration of antibiotic but also depends on the rate of growth of biofilm which was our ultimate goal for the investigation. Through our investigation we are proposing that a slow growing biofilm can be killed by relatively low concentration of antibiotic treatment instead of rigorous antibiotic usage. Although our simulations was not validated with experimental results, but it enlightens resistance mechanism of the biofilm.

References

- [1] D. C. Ellwood, P. D. Marsh, C. M. Brown, J. D. Wardell, and N. Le Roux. Surface-associated growth. *Philos Trans R Soc Lond B Biol Sci*, 297(1088), (2004) 517–532.
- [2] B. Heffernan, C. D. Murphy, and E. Casey. Comparison of planktonic and biofilm cultures of *Pseudomonas fluorescens* DSM 8341 cells grown on fluoroacetate. *Appl Environ Microbiol*, 75(9), (2009) 2899–907.
- [3] D. R. M. Biofilms and device-associated infections. *Emerg Infect Dis*, 7(2), (2001) 277–81.
- [4] A. K. Deva, J. Adams, and K. Vickery. The role of bacterial biofilms in device-associated infection. *Plast Reconstr Surg*, 132(5), (2013) 1319–28.
- [5] R. M. Donlan, J. Adams, and K. Vickery. Biofilms: microbial life on surfaces. *Emerg Infect Dis*, 8(9), (2002) 881–90.
- [6] W. Costerton, R. Veeh, M. Shirtliff, M. Pasmore, C. Post, and G. Ehrlich. The application of biofilm science to the study and control of chronic bacterial infections. *J Clin Invest*, 112(10), (2003) 1466–77.
- [7] S. J. Vandecasteele, W. E. Peetermans, R. Merckx, and J. V. Eldere. Expression of biofilm-associated genes in *Staphylococcus epidermidis* during in vitro and in vivo foreign body infections. *J Infect Dis*, 188(5), (2003) 730–7.
- [8] K. K. Jefferson. What drives bacteria to produce a biofilm? *FEMS Microbiol Lett*, 236(2), (2004) 163–73.
- [9] G. Cappelli, C. Tetta, and B. Canaud. Is biofilm a cause of silent chronic inflammation in haemodialysis patients? A fascinating working hypothesis. *Nephrol Dial Transplant*, 20(2), (2005) 266–70.
- [10] J. W. Costerton. Introduction to biofilm. *Int J Antimicrob Agents*, 11(3-4), (1999) 217–21.
- [11] P. Stoodley, I. Dodds, J. D. Boyle, and H. M. Lappin-Scott. Influence of hydrodynamics and nutrients on biofilm structure. *J Appl Microbiol*, 85 Suppl1, (1998) 19S–28S.
- [12] T. F. C. Mah and G. A. O’Toole. Mechanisms of biofilm resistance to antimicrobial agents. *Trends in microbiology*, 9(1), (2001) 34–39.
- [13] H. C. Flemming and J. Wingender. The biofilm matrix. *Nat Rev Microbiol*, 8(9), (2010) 623–33.

- [14] T. Coenye and H. J. Nelis. In vitro and in vivo model systems to study microbial biofilm formation. *J Microbiol Methods*, 83(2), (2010) 89–105.
- [15] D. G. Maki and P. A. Tambyah. Engineering out the risk for infection with urinary catheters. *Emerg Infect Dis*, 7(2), (2001) 342–7.
- [16] Q. M. Parks, R. L. Young, K. R. Poch, K. C. Malcolm, M. L. Vasil, and J. A. Nick. Neutrophil enhancement of *Pseudomonas aeruginosa* biofilm development: human F-actin and DNA as targets for therapy. *J Med Microbiol*, 58(Pt 4), (2009) 492–502.
- [17] M. Kostakioti, M. Hadjifrangiskou, and S. J. Hultgren. Bacterial biofilms: development, dispersal, and therapeutic strategies in the dawn of the postantibiotic era. *Cold Spring Harb Perspect Med*, 3(4), (2013) a010,306.
- [18] J. S. Webb, L. S. Thompson, S. James, T. Charlton, T. T. Nielsen, B. Koch, M. Givskov, and S. Kjelleberg. Cell death in *Pseudomonas aeruginosa* biofilm development. *J Bacteriol*, 185(15), (2003) 4585–92.
- [19] L. J. Wang, Y. Sun, W. L. Song, Z. J. Zhang, and C. F. Liu. [Changes of drug-resistance of *Pseudomonas aeruginosa* in pediatric intensive care unit]. *Zhonghua Er Ke Za Zhi*, 50(9), (2012) 657–63.
- [20] S. M. Kirov, J. S. Webb, C. Y. O’May, D. W. Reid, J. K. K. Woo, S. A. Rice, and S. Kjelleberg. Biofilm differentiation and dispersal in mucoid *Pseudomonas aeruginosa* isolates from patients with cystic fibrosis. *Microbiology*, 153(Pt 10), (2007) 3264–74.
- [21] T. S. Walker, K. L. Tomlin, G. S. Worthen, K. R. Poch, J. G. Lieber, M. T. Saavedra, M. B. Fessler, K. C. Malcolm, M. L. Michael L. Vasil, and J. A. Nick. Enhanced *Pseudomonas aeruginosa* biofilm development mediated by human neutrophils. *Infect Immun*, 73(6), (2005) 3693–701.
- [22] C. Rollet, L. Gal, and J. Guzzo. Biofilm-detached cells, a transition from a sessile to a planktonic phenotype: a comparative study of adhesion and physiological characteristics in *Pseudomonas aeruginosa*. *FEMS Microbiol Lett*, 290(2), (2009) 135–42.
- [23] F. Gomes, P. Teixeira, H. Ceri, and R. Oliveira. Evaluation of antimicrobial activity of certain combinations of antibiotics against in vitro *Staphylococcus epidermidis* biofilms. *Indian J Med Res*, 135(4), (2012) 542–7.
- [24] T. P. Lim, W. Lee, T. Y. Tan, S. Sasikala, J. Teo, L. Y. Hsu, T. T. Tan, N. Syahidah, and A. L. Kwa. Effective antibiotics in combination against extreme drug-resistant *Pseudomonas aeruginosa* with decreased susceptibility to polymyxin B. *PLoS One*, 6(12), (2011) e28,177.
- [25] H. C. Flemming and J. Wingender. Relevance of microbial extracellular polymeric substances (EPSs)—Part I: Structural and ecological aspects. *Water Sci Technol*, 43(6), (2001) 1–8.
- [26] C. Picioreanu, van Loosdrecht M C, and J. J. Heijnen. Mathematical modeling of biofilm structure with a hybrid differential-discrete cellular automaton approach. *Biotechnol Bioeng*, 58(1), (1998) 101–16.

- [27] M. C. M. van Loosdrecht, J. J. Heijnen, H. Eberl, J. Kreft, and C. Picioreanu. Mathematical modelling of biofilm structures. *Antonie Van Leeuwenhoek*, 81(1-4), (2002) 645–56.
- [28] C. G. Kumar and S. K. Anand. Significance of microbial biofilms in food industry: a review. *Int J Food Microbiol*, 42(1-2), (1998) 9–27.
- [29] P. Verhagen, L. D. Gelder, S. Hoefman, P. D. Vos, and N. Boon. Planktonic versus biofilm catabolic communities: importance of the biofilm for species selection and pesticide degradation. *Appl Environ Microbiol*, 77(14), (2011) 4728–35.
- [30] R. Singh, D. Paul, and R. K. Jain. Biofilms: implications in bioremediation. *Trends Microbiol*, 14(9), (2006) 389–97.
- [31] C. Nicolella, M. C. van Loosdrecht, and S. J. Heijnen. Particle-based biofilm reactor technology. *Trends Biotechnol*, 18(7), (2000) 312–20.
- [32] I. Chang, E. S. Gilbert, N. Eliashberg, and J. D. Keasling. A three-dimensional, stochastic simulation of biofilm growth and transport-related factors that affect structure. *Microbiology*, 149(Pt 10), (2003) 1859–71.
- [33] G. E. Pizarro, C. Garca, R. Moreno, and M. E. Seplveda. Two-dimensional cellular automaton model for mixed-culture biofilm. *Water Sci Technol*, 49(11-12), (2004) 139–8.
- [34] C. S. Laspidou and B. E. Rittmann. Modeling the development of biofilm density including active bacteria, inert biomass, and extracellular polymeric substances. *Water Res*, 38(14-15), (2004) 3349–61.
- [35] C. Picioreanu, J. U. Kreft, and M. C. Van Loosdrecht. Particle-based multidimensional multi-species biofilm model. *Appl Environ Microbiol*, 70(5), (2004) 3024–40.
- [36] L. Hall-Stoodley, J. W. Costerton, and P. Stoodley. Bacterial biofilms: from the natural environment to infectious diseases. *Nat Rev Microbiol*, 2(2), (2004) 95–108.
- [37] B. Purevdorj, J. W. Costerton, and P. Stoodley. Influence of hydrodynamics and cell signaling on the structure and behavior of *Pseudomonas aeruginosa* biofilms. *Appl Environ Microbiol*, 68(9), (2002) 4457–64.
- [38] J. D. Chambless, S. M. Hunt, and P. S. Stewart. A three-dimensional computer model of four hypothetical mechanisms protecting biofilms from antimicrobials. *Appl Environ Microbiol*, 72(3), (2006) 2005–13.
- [39] G. Batoni, G. Maisetta, F. L. Brancatisano, and M. Campa. Use of antimicrobial peptides against microbial biofilms: advantages and limits. *Curr Med Chem*, 18(2), (2011) 256–79.
- [40] A. A. Bahar, D. Ren, and R. K. Jain. Antimicrobial peptides. *Pharmaceuticals (Basel)*, 6(12), (2013) 1543–75.
- [41] Y. Davit, H. Byrne, J. Osborne, J. Pitt-Francis, D. Gavaghan, and M. Quintard. Hydrodynamic dispersion within porous biofilms. *Phys Rev E Stat Nonlin Soft Matter Phys*, 2(2), (2013) 012,718.

- [42] D. Davies. Understanding biofilm resistance to antibacterial agents. *Nat Rev Drug Discov*, 2(2), (2003) 114–22.
- [43] M. G. Dodds, K. J. Grobe, and P. S. Stewart. Modeling biofilm antimicrobial resistance. *Biotechnol Bioeng*, 68(4), (2000) 456–65.
- [44] J. N. Anderl, M. J. Franklin, and S. P. S. Role of antibiotic penetration limitation in *Klebsiella pneumoniae* biofilm resistance to ampicillin and ciprofloxacin. *Antimicrob Agents Chemother*, 44(7), (2000) 1818–24.
- [45] J. B. Kaplan. Biofilm dispersal: mechanisms, clinical implications, and potential therapeutic uses. *J Dent Res*, 89(3), (2010) 205–18.
- [46] C. Picioreanu, M. C. Van Loosdrecht, and H. J. J. Effect of diffusive and convective substrate transport on biofilm structure formation: a two-dimensional modeling study. *Biotechnol Bioeng*, 69(5), (2000) 504–15.
- [47] J.-U. Krefta, C. Picioreanu, J. W. T. Wimpenny, and M. C. M. van Loosdrecht. Individual-based modelling of biofilms. *Microbiology*, 147(Pt 11), (2001) 2897–912.
- [48] M. G. Fagerlind, J. S. Webb, N. Barraud, D. McDougald, A. Jansson, P. Nilsson, M. Haralen, S. Kjelleberg, and S. A. Rice. Dynamic modelling of cell death during biofilm development. *Theor Biol*, 295, (2012) 23–36.
- [49] J. Kim, H.-S. Kim, S. Han, J.-Y. Lee, O. Jae-Eung, S. Chung, and H.-D. Park. Hydrodynamic effects on bacterial biofilm development in a microfluidic environment. *Lab Chip*, 13(10), (2013) 1846–9.
- [50] E. Alpkvist, C. Picioreanu, M. C. M. van Loosdrecht, and A. Heyden. Three-dimensional biofilm model with individual cells and continuum EPS matrix. *Biotechnol Bioeng*, 94(5), (2006) 961–79.
- [51] J. U. Kreft, G. Booth, and W. J. W. BacSim, a simulator for individual-based modelling of bacterial colony growth. *Microbiology*, 144(Pt 12), (1998) 3275–87.
- [52] H. S. W. Two-dimensional simulations of biofilm development: effects of external environmental conditions. *Water Science and Technology*, 39(7), (1999) 107–114.
- [53] P. S. Stewart. Diffusion in biofilms. *J Bacteriol*, 185(5), (2003) 1485–91.
- [54] P. Stoodley, S. Wilson, L. Hall-Stoodley, J. D. Boyle, H. M. Lappon-Scott, and J. W. Costerton. Growth and detachment of cell clusters from mature mixed-species biofilms. *Appl Environ Microbiol*, 67(12), (2001) 5608–13.
- [55] C. Picioreanu, M. C. van Loosdrecht, and J. J. Heijnen. Biofilms: implications in bioremediation. *Biotechnol Bioeng*, 72(2), (2001) 205–18.
- [56] N. G. Cogan and K. J. P. The role of the biofilm matrix in structural development. *Math Med Biol*, 21(2), (2004) 147–66.

- [57] H. C. Flemming, T. R. Neu, and D. J. Wozniak. The EPS matrix: the "house of biofilm cells". *J Bacteriol*, 189(22), (2007) 7945–7.
- [58] A. M. Spormann. Physiology of microbes in biofilms. *Curr Top Microbiol Immunol*, 322, (2008) 17–36.
- [59] P. Watnick and R. Kolter. Biofilm, city of microbes. *J Bacteriol*, 182(10), (2000) 2675–9.
- [60] J. Xiao, M. L. Klein, M. L. Falsetta, B. Lu, C. M. Delahunty, J. R. Yates, A. Heydorn, and H. Koo. The exopolysaccharide matrix modulates the interaction between 3D architecture and virulence of a mixed-species oral biofilm. *PLoS Pathog*, 8(4), (2012) e1002623.
- [61] J. A. Fozard, M. Lees, J. R. King, and B. S. Logan. Inhibition of quorum sensing in a computational biofilm simulation. *Biosystems*, 109(2), (2012) 105–14.
- [62] C. M. Waters and B. L. Bassler. Quorum sensing: cell-to-cell communication in bacteria. *Annu Rev Cell Dev Biol*, 21, (2005) 319–46.
- [63] B. R. Boles and A. R. Horswill. Agr-mediated dispersal of *Staphylococcus aureus* biofilms. *PLoS Pathog*, 4(4), (2008) e1000052.
- [64] J. M. Yarwood, D. J. Bartels, E. M. Volper, and E. P. Greenberg. Quorum sensing in *Staphylococcus aureus* biofilms. *J Bacteriol*, 186(6), (2004) 838–50.
- [65] C. D. Sifri. Healthcare epidemiology: quorum sensing: bacteria talk sense. *Clin Infect Dis*, 47(8), (2008) 1070–6.
- [66] N. G. Cogan, R. Cortez, and L. Fauci. Modeling physiological resistance in bacterial biofilms. *Bull Math Biol*, 67(4), (2005) 831–53.
- [67] P. S. Stewart. Biofilm accumulation model that predicts antibiotic resistance of *Pseudomonas aeruginosa* biofilms. *Antimicrob Agents Chemother*, 38(5), (1994) 1052–8.
- [68] A. Varaiya, K. Nikhil, K. Manasi, B. Pallavi, and D. Jyotsana. Incidence of metallo beta lactamase producing *Pseudomonas aeruginosa* in ICU patients. *Indian J Med Res*, 127(4), (2004) 398–402.